Direct Observation of a Lattice-Framework Silylene: A Planar Four-Membered-Ring Dialkylsilylene with a Small HOMO−LUMO Energy Gap

Eunsang Kwon,*,† Hiromasa Tanaka,† Takayuki Makino,† Shinobu Tsutsui,† Shigeki Matsumoto,† Yusaburo Segawa,† and Kenkichi Sakamoto*,†,‡

Photodynamics Research Center, The Institute of Physical and Chemical Research (RIKEN), 519-1399 Aoba, Aramaki, Aoba-ku, Sendai 980-0845, Japan, and Department of Chemistry, Graduate School of Science, Tohoku University, Aoba-ku, Sendai 980-8578, Japan

Received August 15, 2005

Summary: The n−p transition of the lattice-framework silylene 2,3,4,6,7,8-hexa-tert-butyl-1,5-disilatricyclo[4.2.0.0^{1,4}]octa-2,7-diene-5,5-diyl was observed by differential transmission spectroscopy at 764 nm. The significantly red-shifted n−p transition of the silylene is caused by the planar four-membered Si_2C_2 ring containing the divalent silicon atom.

Introduction

Electronic absorption spectra have been reported for a variety of silylene derivatives in argon or hydrocarbon matrices since the first direct observation of an organosilylene, dimethylsilylene (**1**; λ_{max} = 453 nm), in a 3-methylpentane (3-MP) glass matrix at 77 K by West and co-workers in 1979.[1,2] The longest wavelength absorption band of the silylenes is generally assignable to the n−p (HOMO−LUMO) transition, which is strongly influenced by the substituents on the silicon atom. Recently, Kira et al. reported the first isolated dialkylsilylene, 2,2,5,5-tetrakis(trimethylsilyl)-1-silacyclopentane-1,1-diyl (**2**), whose n−p transition was measured to be 440 nm in hexane at room temperature.[3]

Very recently, we reported the thermal equilibrium of the unique lattice-framework dialkylsilylene **3** with the corresponding disilene **4** (eq 1).[4] Our interest lay in whether the HOMO−LUMO transition of **3** would be influenced by its structure, because **4** has a significantly red-shifted HOMO−LUMO transition originating from its unique molecular structure.[4c] We initially examined the photolysis of **4** in a 3-MP glass matrix at low temperature, because the dissociation of **4** was significantly activated by irradiation with visible light.[4b] However, upon irradiation using an ultra-high-pressure mercury lamp at 77 K, we did not observe the generation of **3** by UV/vis spectroscopy. This result indicates that the photochemically generated **3** is rapidly dimerized into **4** even at low temperatures and/or that the sensitivity of the method is inadequate for observing **3**. Thus, to observe **3**, we employed differential transmission (DT) spectroscopy using the lock-in technique[5] combined with the laser photolysis of **4**. This method is sufficiently sensitive to observe such transient species with a sufficient signal to noise ratio. In addition, this method is suitable for observing such a silylene, since photoirradiation accelerated the dissociation of **4** to **3**. This paper reports the direct observation of **3** with a very small HOMO−LUMO energy gap. Time-dependent density-functional theory (TD-DFT)[6,7] calculations strongly support the experimental results. To elucidate the origin of the small n−p transition energy of **3**, the HOMO and LUMO energies of **3** were calculated and compared with those of model silylenes. The singlet−triplet energy gap of **3** was also estimated by DFT calculations.

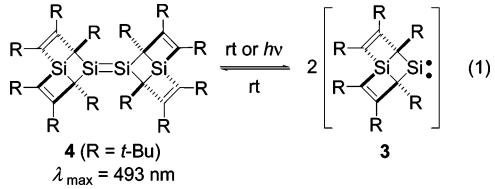

4 (R = *t*-Bu)
λ_{max} = 493 nm

3

Results and Discussion

The generation of **3** by laser photolysis was confirmed by chemical trapping experiments. Upon the photolysis of **4** with

* To whom correspondence should be addressed. E-mail: ekwon@riken.jp (E.K.); sakamoto@mail.tains.tohoku.ac.jp (K.S.).

† RIKEN.

‡ Tohoku University.

(1) For recent reviews on silylenes, see: (a) Apeloig, Y. In *The Chemistry of Organic Silicon Compounds*; Patai, S., Rappoport, Z., Eds.; Wiley: New York, 1989; Part 1, Chapter 2. (b) Gaspar, P. P.; West, R. In *The Chemistry of Organic Silicon Compounds II*; Rappoport, Z., Apeloig, Y., Eds.; Wiley: New York, 1998; Vol. 2, Part 3, Chapter 43. (c) Haaf, M.; Schmedake, T. A.; West, R. *Acc. Chem. Res.* **2000**, *33*, 704. (d) Tokitoh, N.; Okazaki, R. *Coord. Chem. Rev.* **2000**, *210*, 251. (e) Gehrhus, B.; Lappert, M. F. *J. Organomet. Chem.* **2001**, *617*, 209. (f) Gaspar, P. P.; Xiao, M.; Pae, D. H.; Berger, D. J.; Haile, T.; Chen, T.; Lei, D.; Winchester, W. R.; Jiang, P. *J. Organomet. Chem.* **2002**, *646*, 68. (g) Kira, M. *J. Organomet. Chem.* **2004**, *689*, 1337.

(2) Drahnak, T. J.; Michl, J.; West, R. *J. Am. Chem. Soc.* **1979**, *101*, 5427.

(3) Kira, M.; Ishida, S.; Iwamoto, T.; Kabuto, C. *J. Am. Chem. Soc.* **1999**, *121*, 9722.

(4) (a) Matsumoto, S.; Tsutsui, S.; Kwon, E.; Sakamoto, K. *Angew. Chem., Int. Ed.* **2004**, *43*, 4610. (b) Tsutsui, S.; Tanaka, H.; Kwon, E.; Matsumoto, S.; Sakamoto, K. *Organometallics* **2004**, *23*, 5659. (c) Tanaka, H.; Kwon, E.; Tsutsui, S.; Matsumoto, S.; Sakamoto, K. *Eur. J. Inorg. Chem.* **2005**, 1235. (d) Tsutsui, S.; Tanaka, H.; Kwon, E.; Matsumoto, S.; Sakamoto, K. *Organometallics* **2005**, *24*, 4629.

(5) Cardona, M. In *Modulation Spectroscopy*; Academic Press: New York, 1969.

(6) Frisch, M. J.; Trucks, G. W.; Schlegel, H. B.; Scuseria, G. E.; Robb, M. A.; Cheeseman, J. R.; Zakrzewski, V. G.; Montgomery, J. A., Jr.; Stratmann, R. E.; Burant, J. C.; Dapprich, S.; Millam, J. M.; Daniels, A. D.; Kudin, K. N.; Strain, M. C.; Farkas, O.; Tomasi, J.; Barone, V.; Cossi, M.; Cammi, R.; Mennucci, B.; Pomelli, C.; Adamo, C.; Clifford, S.; Ochterski, J.; Petersson, G. A.; Ayala, P. Y.; Cui, Q.; Morokuma, K.; Malick, D. K.; Rabuck, A. D.; Raghavachari, K.; Foresman, J. B.; Cioslowski, J.; Ortiz, J. V.; Stefanov, B. B.; Liu, G.; Liashenko, A.; Piskorz, P.; Komaromi, I.; Gomperts, R.; Martin, R. L.; Fox, D. J.; Keith, T.; Al-Laham, M. A.; Peng, C. Y.; Nanayakkara, A.; Gonzalez, C.; Challacombe, M.; Gill, P. M. W.; Johnson, B. G.; Chen, W.; Wong, M. W.; Andres, J. L.; Head-Gordon, M.; Replogle, E. S.; Pople, J. A. *Gaussian 98*, revision A.11; Gaussian, Inc.: Pittsburgh, PA, 1998.

(7) The computational method is based on a DFT calculation with the B3LYP hybrid function. See: (a) Becke, A. D. *J. Chem. Phys.*, **1993**, *98*, 5648. (b) Lee, C.; Yang, W.; Parr, R. *Phys. Rev. B* **1988**, *37*, 785.

10.1021/om0507023 CCC: $33.50
Publication on Web 02/01/2006

the 514.5 nm line from a argon ion laser beam in the presence of bis(trimethylsilyl)acetylene in cyclohexane at room temperature, the silacyclopropene derivative **5**[4b] was quantitatively obtained (Scheme 1). Also, the photolysis of **4** in the presence

Scheme 1

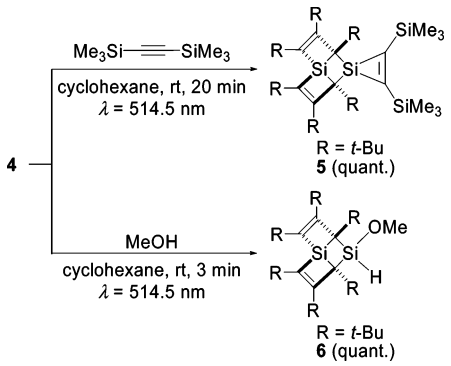

of methanol afforded only the silylene adduct **6**.[4b] Next, we used DT spectroscopy combined with laser photolysis to directly observe **3**.[8] Upon the photolysis of **4** without a trapping reagent, the peak of the DT spectrum was observed at 764 nm, as shown in Figure 1. The laser power dependence of the integral

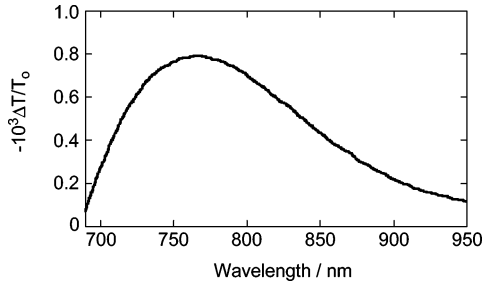

Figure 1. Differential transmission spectrum of our sample measured under laser irradiation conditions (cw, chopped at 1500 Hz, laser power 6 W).

intensities of the signals from 650 to 950 nm is obtained from a straight line with a slope of 1.[8] This result indicates that **4** is dissociated via a one-photon process.

When the irradiation was stopped, the signals immediately disappeared within the time resolution of the measurement. Because **4** was not decomposed after the irradiation, the dimerization of **3** into **4** quantitatively occurred.[9] The experimental results indicate that the peak at 764 nm originates from silylene **3**. If the peak is assigned to the n−p transition of **3**, the transition is largely red shifted relative to 453 nm for **1** and 440 nm for **2**. Therefore, to establish the assignment of the peak, the electron transition energies of **3** were calculated by the time-dependent DFT (TD-DFT)[10,11] method.

The geometric optimization of **3** was carried out at the same theoretical level as employed for disilene **4**.[4b] The optimized structure and selected geometric parameters of **3** are shown in Figure 2. The geometry of the lattice-framework skeleton in **3**

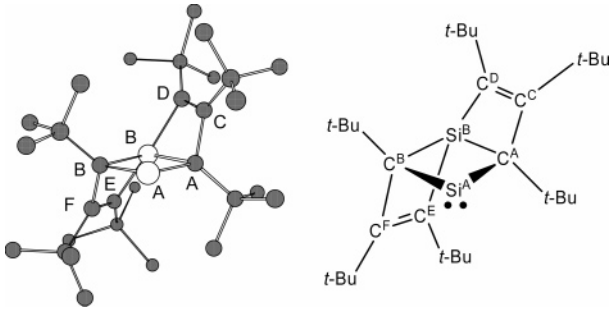

Figure 2. Optimized structure of **3**. Hydrogen atoms are omitted for clarity. Selected bond lengths (Å) and bond angles (deg): Si^A-C^A, 1.984; Si^B-C^B, 1.902; C^A-C^C, 1.576; Si^B-C^D, 1.876; C^C-C^D, 1.381; $C^A-Si^B-C^B$, 87.5; $Si^A-C^A-Si^B$, 90.3; $C^A-Si^B-C^B$, 92.2; $Si^A-C^A-C^C$, 112.3; $C^B-Si^B-C^D$, 125.3; $C^D-Si^B-C^E$, 148.4; $Si^A-C^A-Si^B-C^B$, 1.7.

is very close to that in **4**.[4a] The most striking feature in the geometry of **3** is the planarity of the Si_2C_2 ring including the divalent silicon atom. The $Si^A-C^A-Si^B-C^B$ dihedral angle in **3** (1.7°) is significantly smaller than that in the optimized structure of 1,3-disilacyclobutane-1,1-diyl (25.3°). When the geometric parameters of **3** and **2** are compared, the C−(Si:)−C angle in **3** (87.5°) is smaller than that in **2** (93.88°),[3] while the average C−(Si:) distance in **3** (1.981 Å) is much longer than that in **2** (1.908 Å)[3]. The calculated singlet−triplet energy difference (ΔE_{S-T}) value of **3** is −70 kJ/mol, and thus the singlet state is more stable than the triplet state. This ΔE_{S-T} value is higher than the values of **2** (−135 kJ/mol calculated at the B3LYP/6-311+G(d,p) level) and **1** (−108.1 kJ/mol), while it is much lower than the value for $(t\text{-Bu}_3\text{Si})_2\text{Si}$: (+18.8 kJ/mol calculated at the BLYP/TZVP level).[12,13]

We first examined the applicability of the TD-DFT calculation to silylenes. The electron transition energies for the various reported silylenes were calculated at the TD-B3LYP/6-311+G(d,p) level and were compared with the observed values.[3,14] As shown in Figure 3, a good correlation with a correlation coefficient of 0.98 was found between the observed and calculated values. This indicates that the use of the TD-B3LYP calculation combined with the 6-311+G(d,p) basis set is sufficient for predicting the absorption wavelengths of the silylenes. With the TD-B3LYP/6-311+G(d,p) level, the n−p transition of **3** is calculated to be 811 nm. This result strongly supports the idea that the measured peak at 764 nm stems from the n−p transition of **3**. The calculation result also shows that the n−p transition of **3** is extremely red-shifted relative to that of all the reported dialkylsilylenes.

For the small $\pi-\pi^*$ transition energy of **4**, the lowering of the LUMO energy level is responsible.[4c] This is caused by a through-space interaction between the π^* orbital of the Si═Si bond and the π^* orbital of the four C═C bonds in the lattice-

(8) The experimental arrangement for the measurement of the DT spectrum and the log−log plot of the integral intensity of the signal versus laser power are given in the Supporting Information.

(9) The UV/vis absorption spectra of the sample did not change before and after the laser photolysis.

(10) Takahashi, M.; Kira, M.; Sakamoto, K.; Müller, T.; Apeloig, Y. *J. Comput. Chem.* **2001**, *13*, 1536.

(11) (a) Stratmann, R. E.; Scuseria, G. E.; Frisch, M. J. *J. Chem. Phys.* **1998**, *109*, 8218. (b) Bauernschmitt, R.; Ahlrichs, R. *Chem. Phys. Lett.* **1996**, *256*, 454. (c) Casida, M. E.; Jamorski, C.; Casida, K. C.; Salahub, K. D. R. *J. Chem. Phys.* **1998**, *108*, 4439.

(12) Yoshida, M.; Tamaoki, N. *Organometallics* **2002**, *21*, 2587.

(13) Sekiguchi and co-workers experimentally generated $(t\text{-Bu}_3\text{Si})_2\text{Si}$: and confirmed that the ground state of the silylene is triplet by ESR spectroscopy. Sekiguchi, A.; Tanaka, T.; Ichinohe, M.; Akiyama, K.; Tero-Kubota, S. *J. Am. Chem. Soc.* **2003**, *125*, 4962.

(14) (a) For **7**: Schmedake, T. A.; Haaf, M.; Apeloig, Y.; Müller, T.; Bukalov, S.; West, R. *J. Am. Chem. Soc.* **1999**, *121*, 9479. (b) For **8**: Leites, L. A.; Bukalov, S. S.; Denk, M.; West, R.; Haaf, M. *J. Mol. Struct.* **2000**, *550−551*, 329. (c) For **9**: Gehrhus, B.; Lappert, M. F.; Heinicke, J.; Boese, R.; Bläster, D. *J. Chem. Soc., Chem. Commun.* **1995**, 1931. (d) For **10**: Maier, G.; Reisenauer, H. P.; Pacl, H. *Angew. Chem., Int. Ed. Engl.* **1994**, *33*, 1248. (e) For **11**: Welsh, K. M.; Michl, J.; West, R. *J. Am. Chem. Soc.* **1988**, *110*, 6689. (f) For **12**, **14**, and **15**: Michalczyk, M. J.; Fink, M. J.; De Young, D. J.; Carlson, C. W.; Welsh, K. M.; West, R. *Silicon, Germanium, Tin Lead Compd.* **1986**, *9*, 75. (g) For **13**: West, R.; Fink, M. J.; Michl, J. *Science* **1981**, *214*, 1343.

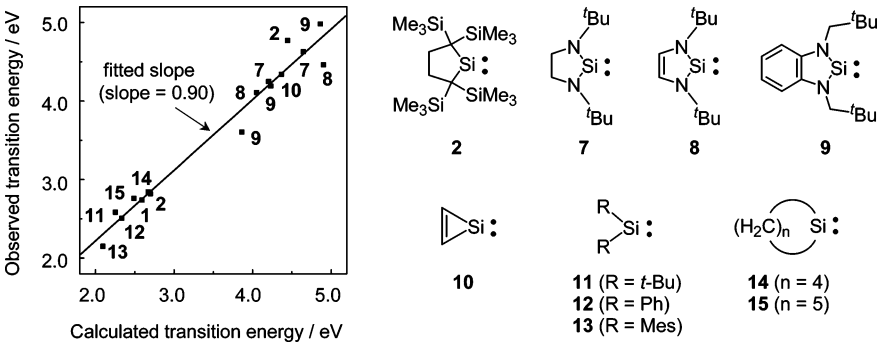

Figure 3. Correlation between observed and calculated transition energies of silylenes at the TD-B3LYP/6-311+G(d,p) level.

Table 1. MO Energies and n−p Transition Energy (TE) of Silylenes Calculated by the TD-B3LYP Method

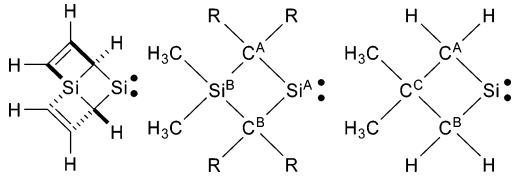

16 **17** (R = CH_3) **18** (R = H) **19**

silylene	HOMO/eV[a]	LUMO/eV[a]	TE/eV[b]
3	−4.73 (0)	−2.21 (0)	1.53 (811)
16-fix	−5.38 (−0.65)	−2.82 (−0.61)	1.58 (787)
17-fix	−5.27 (−0.54)	−2.61 (−0.40)	1.63 (761)
18-fix	−5.42 (−0.69)	−2.62 (−0.41)	1.78 (697)
18-opt	−5.57 (−0.84)	−2.38 (−0.17)	2.26 (548)
19-fix	−5.38 (−0.65)	−2.55 (−0.34)	1.80 (688)
19-opt	−5.70 (−0.98)	−2.46 (−0.25)	2.25 (550)
1-fix	−6.22 (−1.49)	−2.59 (−0.38)	2.73 (454)

[a] The energies relative to the value of **3** are presented in parentheses. [b] The corresponding wavelengths in nm are presented in parentheses.

framework skeleton. What factors control the n−p transition energy of the lattice-framework silylene **3**. To elucidate the origin of the red-shifted n−p transition of **3**, we selected the five model silylenes **1** and **16**−**19** and calculated their n−p transition energies as well as the MO energies (Table 1).

First, the results of the DFT calculations for **3** and **16-fix** are compared in order to evaluate the substituent effects caused by the bulky *tert*-butyl groups. In the structure of silylene **16-fix**, all of the *tert*-butyl groups in **3** are replaced by hydrogen atoms. The geometric parameters for the lattice-framework skeleton of **16-fix** are fixed to those of **3**. The n−p transition energy of **16-fix** (1.58 eV or 787 nm) is almost similar to that of **3** (1.53 eV or 811 nm). Both the HOMO and LUMO energy levels of **16-fix** become lower by ∼0.6 eV relative to those of **3**. The order of the lowering of the MO energy level can be associated with the order of the electron-donating ability of the substituents on the lattice-framework skeleton (*tert*-butyl group > hydrogen atom).[4c] We concluded that the bulkiness of the substituents on the lattice-framework skeleton only slightly affects the n−p transition energy of silylene **3**.

Second, to discuss how the lattice-framework skeleton influences the n−p transition energy and the MO energy levels, the results for **3** are compared with those of **17-fix**, **18-fix**, and **18-opt**. In the structures of silylenes **17** and **18**, two annulated silacyclobutene rings in **3** are broken and are replaced by methyl groups or hydrogen atoms. The geometries of the four-membered Si_2C_2 ring in **17-fix** and **18-fix** are fixed to that in **3**. The lowest energy structure of **18** (**18-opt**) has a bent Si_2C_2 ring, and the $Si^A-C^A-Si^B-C^B$ angle is as large as 24.3°. The n−p transition energies of **17-fix** and **18-fix** are calculated to be 1.63 eV (761 nm) and 1.78 eV (697 nm), respectively, which are relatively close to the value of **3**. In contrast, the n−p transition energy of **18-opt** is calculated to be 2.26 eV (548 nm), which is significantly blue-shifted relative to **18-fix**. The TD calculation suggests that the planarity of the Si_2C_2 ring would strongly influence the n−p transition energy. Removing the annulated cyclobutene rings from the lattice framework only slightly influences the n−p transition energy of the silylenes, unlike the case of the red-shifted $\pi-\pi^*$ transition of disilene **4**.[4c]

Finally, the TD calculations for **1-fix**, **19-fix**, and **19-opt** were performed in order to discuss the role of the sp^3 silicon atom in the red shift of the n−p transition. In the structure of **1-fix**, the bond angle of C−Si−C and the bond lengths of C−Si were fixed to those of **3**. Silylene **19** has a structure in which the sp^3 silicon atom in **18** is replaced by the carbon atom. In the structure of **19-fix**, the geometric parameters for the Si−C bond lengths, the C^A-Si-C^B bond angle, and the $Si-C^A-C^C-C^B$ angle are fixed to those for **3**. The lowest energy structure of **19** (**19-opt**) has a bent SiC_3 ring, and the $Si-C^A-C^C-C^B$ angle is as large as 22.6°. The n−p transition energy of **19-fix** (1.80 eV or 688 nm) is close to that of **18-fix**. The n−p transition energy of **19-opt** was calculated to be 2.25 eV (550 nm), which is comparable to the value of **18-opt**. The n−p transition energy of **1-fix** was calculated to be 2.73 eV (454 nm), which is blue-shifted relative to the value of **18-fix**. The calculation results for **1**, **18**, and **19** suggest that the formation of the planar four-membered ring plays a major role in the small n−p transition energy of the lattice-framework silylene.[15] It is notable that the difference in total energies between **18-fix** and **18-opt** is 9.9 kJ/mol, while the difference between **19-fix** and **19-opt** is 159.9 kJ/mol. This indicates that the SiC_3 ring requires a very large energy to be planar compared with the Si_2C_2 ring. Thus, the sp^3 silicon atom in **3** *geometrically* contributes to the red-shifted n−p transition. When the HOMO and LUMO energies of **17-fix**, **18-fix**, and **1-fix** are compared, the HOMO energy level significantly changes between **18-fix** and **1-fix**, while the LUMO energy level changes to a small degree among the three silylenes. This means that the atom in the four-membered ring opposite to the divalent silicon atom strongly affects the stability of the HOMO.

The orbital correlation diagram shown in Figure 4 provides a useful insight into understanding the difference in the MO energies between **18-fix** and **1-fix**. In Figure 4, **18-fix** is

(15) A four-membered-ring silylene especially has a small n−p transition energy, even if it has a nonplanar geometry. The n−p transition energies of silylenes having a cyclo-$(H_2C)_n$Si: ($n = 2-5$) ring structure are calculated to be as follows: 2.37 eV (524 nm) for cyclo-$(H_2C)_2$Si:, 2.19 eV (565 nm) for cyclo-$(H_2C)_3$Si:, 2.67 eV (464 nm) for cyclo-$(H_2C)_4$Si: (**14**), and 2.49 eV (498 nm) for cyclo-$(H_2C)_5$Si: (**15**).

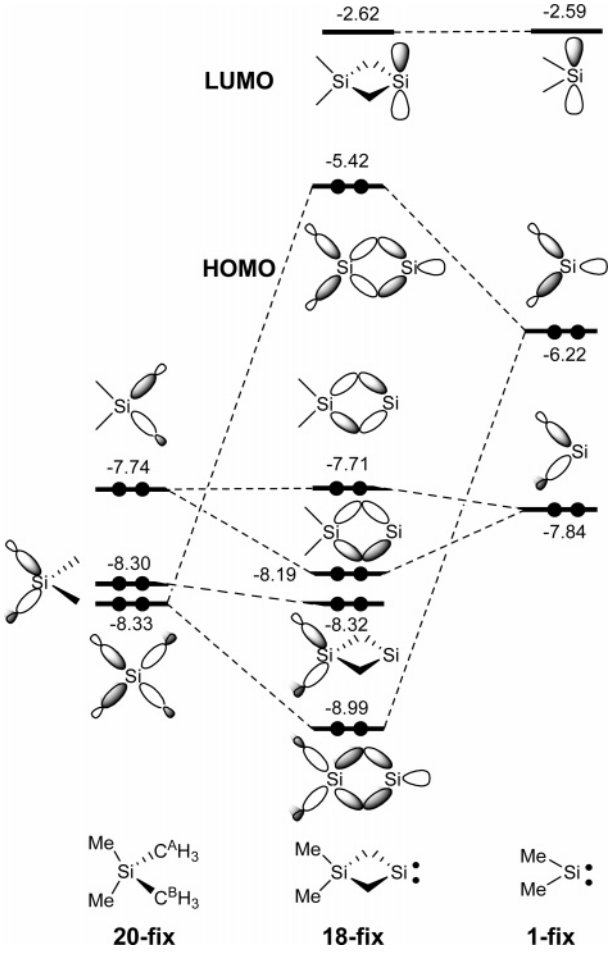

Figure 4. Orbital correlation diagram for **18-fix**, based on B3LYP/6-311+G(d,p) calculations.

tentatively divided into two fragments: the dimethylsilylene **1-fix** and tetramethylsilane **20-fix**, in which the Si−C^A (Si−C^B) bond distance and the C^A−Si−C^B bond angle are fixed to those of **3**. For the occupied MOs, three σ(Si−C) orbitals of **20-fix** correlate with two MOs of **1-fix** to form five MOs of **18-fix**. The correlation between the HOMO of **20-fix** and the HOMO-1 of **1-fix** produces the HOMO-1 and HOMO-2 of **18-fix**. The HOMO-1 of **20-fix** does not interact with the two occupied MOs of **1-fix** and consequently gives the HOMO-3 of **18-fix**. The HOMO-2 of **20-fix** correlates with the HOMO of **1-fix** to generate the HOMO and the HOMO-4 of **18-fix**. This correlation provides the higher energy level of the HOMO of **18-fix** compared with that of **1-fix**. The interaction between the LUMOs of **1-fix** and **20-fix** is almost negligible, because the LUMO energy of **20-fix** (−0.31 eV) is very high. Thus, the LUMO energies of **1-fix** and **18-fix** are comparable. In summary, the correlation between the σ(Si−C) orbitals in the Si_2C_2 ring and the nonbonding orbital of the divalent silicon atom destabilizes the HOMO of **3**, resulting in the significantly small HOMO−LUMO energy gap.

In conclusion, we observed the n−p transition of **3** at 764 nm (1.62 eV) using DT spectroscopy. This absorption wavelength is significantly red-shifted relative to the other reported dialkylsilylenes. DFT calculations revealed that the small n−p transition energy of **3** is caused by the planar four-membered Si_2C_2 ring including the divalent silicon atom.

Experimental Section

General Methods. ^{1}H NMR spectra were recorded on a Varian INOVA 300 FT-NMR spectrometer at 300 MHz. Electronic absorption spectra were recorded on an Agilent 8453 UV−visible spectrometer. The instruments used for measurement of the differential transmission spectrum: Ar-ion laser, Spectra-physics Model 2040E; monochromator, Acton Research Corporation Spectra Pro-300i; light source, Philips tungsten lamp 150W/24V; detector, Hamamatsu Photonics Si-PIN photodiode C1808-03.

Materials. Cyclohexane was degassed and distilled over potassium. Bis(trimethylsilyl)acetylene was commercially available and was used as supplied. Anhydrous Methanol (Aldrich Chemical Co.) was degassed by three freeze−pump−thaw cycles before use.

Photolysis of 4 in the Presence of Bis(trimethylsilyl)acetylene. A dry cyclohexane (2 mL) solution of **4** (6.70 mg, 7.1×10^{-6} mol) with bis(trimethylsilyl)acetylene (24.2 mg, 0.14 mmol) was sealed in a quartz cell (10 mm × 10 mm) under an argon atmosphere. Photolysis of the sample with the 514.5 nm line of a laser beam (cw, laser power 6 W) for 20 min gave **5** quantitatively, as determined by ^{1}H NMR spectroscopy.

Photolysis of 4 in the Presence of Methanol. A dry cyclohexane (2 mL) solution of **4** (6.70 mg, 7.1×10^{-6} mol) with methanol (2 mg, 6.2×10^{-5} mol) was sealed in a quartz cell (10 mm × 10 mm) under an argon atmosphere. Photolysis of the sample with the 514.5 nm line of a laser beam (cw, laser power 6 W) for 3 min gave **6** quantitatively, as determined by ^{1}H NMR spectroscopy.

Differential Transmission Spectra. As a sample for the measurement of the differential transmission spectra, a dry cyclohexane (2 mL) solution of **4** (6.70 mg, 7.1×10^{-6} mol) was sealed in a quartz cell (10 mm × 10 mm) under an argon atmosphere. The experimental setup for the measurement of the differential transmission spectra was similar to that in the literature.[5] A laser beam chopped at 1500 Hz was used as the light for photolysis, the output power of which was varied from 1 to 8 W. The light for the detection from a monochromatized tungsten lamp was irradiated onto the sample cell. To obtain a sufficient signal-to-noise ratio, quasi-multiple-path geometry was adopted; namely, the probe beam was transmitted through the cell three times. The DT spectra were measured in the 650−950 nm wavelength range using a grating spectrometer 30 cm in length and an Si-PIN photodiode. All of the measurements were performed at room temperature.

Theoretical Calculations. All calculations were carried out using the Gaussian98 program.[6] For the optimization of **3**, the following basis sets were employed: The 3-21G basis set was employed for the *tert*-butyl groups and the 6-31G basis set for the other atoms. The other compounds were optimized at the B3LYP/6-311+G(d,p) level. The single-point energy calculations and TD-DFT[9,10] calculations of all compounds were performed at the B3LYP/6-311+G(d,p) level.

Supporting Information Available: Tables giving the Cartesian coordinates of the silylenes presented in this study and figures of the experimental arrangement for the measurement of the DT spectrum and the log−log plot of the integral intensity of the signal versus laser power for our samples. This material is available free of charge via the Internet at http://pubs.acs.org.

OM0507023